EXERGY DESTRUCTION RATE MINIMIZATION IN THE ABSORBER OF A DOUBLE EFFECT VAPOR ABSORPTION SYSTEM

by

Muhammad Usman MUSHTAQ[a,b], Muhammad Sajid KAMRAN[b],
Haseeb YAQOOB[a], Muhammad Ahmad JAMIL[a], Muhammad Basit SHAFIQ[a],
Tauseef REHMAN[c], and Hafiz Muhammad ALI[d,e]*

[a] Department of Mechanical Engineering,
Khwaja Fareed University of Engineering and Information Technology, Rahim Yar Khan, Pakistan
[b] Faculty of Engineering, University of Engineering and Technology, Lahore, Pakistan
[c] Mechanical Engineering Department,
Quaid-e-Azam College of Engineering and Technology, Sahiwal, Pakistan
[d] Mechanical Engineering Department, King Fahd University of Petroleum and Minerals,
Dhahran, Saudi Arabia
[e] Interdisciplinary Research Center for Renewable Energy and Power Systems (IRC-REPS),
King Fahd University of Petroleum and Minerals, Dhahran, Saudi Arabia

Original scientific paper
https://doi.org/10.2298/TSCI201016222M

Despite the wide applications of multi-effect vapor absorption systems, their energy requirement is relatively higher. Also, their exergy analyses found in the literature reveal that the exergy destruction rate at the absorber is quite significant and has the potential for improvement in its energy efficiency. In this work, the exergy destruction rate at the absorber is minimized using the penalty factor method against the optimized generator temperature of the double-effect vapor absorption system by considering absorber, evaporator, and condenser temperatures into consideration. Modeling of the double-effect vapor absorption system was performed using a thermodynamic toolbox in SIMULINK. The present model employed a refrigerant heat exchanger to enhance the system cooling capacity. The liquid-vapor ejector valve at the absorber also improved the mixing of the solution and refrigerant vapor resulting in lower irreversibility of the system. Results show that the coefficient of a performance increase by 2.4% with refrigerant heat exchanger and exergy loss at absorber decrease by 9.4% with ejector. The optimum performance was seen at the condenser and evaporator temperatures of 308.8 K and 278.1 K, respectively with an 8.2% improvement in exergetic efficiency. Finally, it is concluded that the multi-effect absorption system shows better performance by minimizing the irreversibility.

Key words: *exergy destruction rate, LiBr-H_2O, penalty factor method,*
double effect vapor absorption system, cut-off temperature

Introduction

Energy markets in the world are in a state of change and the energy demand is intensifying around the globe. As stated by the International Energy Outlook 2017 (IEO2017), between 2015 and 2040, world energy utilization expands by 28% with more than half of the increase attributed to non-OECD Asian countries. International Finance Corporation market study

---

* Corresponding author, e-mail: hafiz.ali@kfupm.edu.sa

declares that the total energy savings potential in Pakistan is 17.25%. Johnson Control tells us in a report of energy consumption and heat recovery of the refrigeration system, 45% of energy is used for refrigeration in a domain or an arena, [1]. Florides *et al.* [2] modeled the absorption solar cooling system and they calculated the total equivalent warming impact (TEWI) of the system and found that it has a lower TEWI being 1.2 times smaller as compared to the vapor compression system. The further thermal energy storage capacity of the building can be improved by adding phase change materials in glazing structures [3, 4]. In a comparative study of different combinations of the refrigerant-absorbent, Siddiqui [5] found that the operating cost of the LiBr-H_2O cycle is the lowest. Asdrubali and Grignaffini [6] and Kumar *et al.* [7] calculated the working of the single-effect absorption machine. Their experimental work shows that the absorption machine can operate with acceptable efficiency, with an input temperature of 65-70 ^oC at the generator. Farshi *et al.* [8] executed the analysis of the combined ejector-absorption single effect system and concluded that a single effect vapor absorption system (VAS) with ejector before the absorber exhibit relative low exergy loss at the absorber. Various approaches are reported in the literature for using a liquid-vapor ejector at the entrance of the absorber to decrease losses of energy [8-10]. Chen [11] also presented and analyzed the modified ejector-absorber absorption refrigeration cycle and get improvement in COP for refrigerant R-22 at the 0.5 effectiveness of heat exchanger (HE).

Azhar and Siddiqui [12] state that the multi-effect absorption cycle is more beneficial because it results in high COP. Gomri and Hakimi [13] performed the Second law analysis of the double-effect absorption refrigeration system. Results facilitate the identification of system components with high exergy loss. Exergy analysis of the system operating with LiBr-H_2O shows that absorber has the highest exergy loss rate. Khaliq and Kumar [14] performed the exergy analysis of double-effect vapor absorption system (DVAS). During exergy analysis of single effect and multi-effect VAS, it is found that exergy loss is maximum at absorber resulting high value of irreversibility. Arora and Kaushik [15] stated that energy efficiency and COP are inter-related to absorber temperature as well. Exergy efficiency can be improved by optimizing the operating conditions as performed by Rostami *et al.* [16]. Exergy destruction within the system is due to the irreversibilities of the system [17]. Ben Jemaa *et al.* [18] described the exergy destruction rate and stated that the exergy destruction rate at the solution side is 74% of the total while too much in absorber (relative irreversibility 36%). As refrigerant vapors emitting from evaporator enters absorber, entropy generation is too much due to the high temperature difference between the refrigerant and outer circuit cooling water. This fact causes more exergy destruction rate at absorber making absorber less efficient component of VAS. Exergy analysis offers more justifiable facts and figures while weighing the performance of any thermodynamic system. Azhar and Siddiqui [19] performed the energy and exergy analysis for optimization of the operating temperatures. Rostamzadeh *et al.* [20] performed the exergoeconomic analysis and optimized the performance of the combined power and refrigeration cycle. There exist maximum COP and maximum exergetic efficiency as the temperature in the secondary generator and main generator varied, thus leading to optimum operating temperature for the absorption system. This temperature increases with an increase in condenser and absorber temperature. Pandya *et al.* [21] stated that cut-off temperature increases with an increase in absorber temperature. Because the mass concentration of LiBr in solution increases contributing to the higher value of cut-off temperature. At lower generator temperature, COP and exergy efficiency of the cycle improved as compared to classic absorption refrigeration cycles by using an ejector as performed by Sozen and Ozalp [10]. The present model regulates the irreversibility of the system by implying the refrigerant heat exchanger and liquid-vapor ejector before the refrigerant enters the absorber. The use of refrigerant heat exchanger (RHE) also improved the COP 3% as compared to previous work by lowering the temperature in the evaporator to 5.2 °C. Moreover, improvements are obtained by amending the temperatures at the evaporator and condenser by using an optimization technique of the penalty factor method (PFM) [22].

The DVAS model description

The DVAS system model operates with three distinct levels of pressure. Generator, g, operates with high temperature and high pressure while secondary generator, g_{sec}, and condenser, c, conduct the processes with medium pressure. Evaporator, e, ejector valve, E_{v} and absorber, a, complete the processes with low pressure in the DVAS system. Primary generator, secondary generator, and condenser are single-pass horizontal tube HE. A strong solution moves to the primary generator after passing through the solution HE. A high temperature heat source [23] provides heat to the primary generator to produce refrigerant vapors. The weak solution at the outlet of the generator enters the secondary generator subsequently passing the solution heat exchanger, HE2. In the secondary generator, water vapors coming out of the primary generator produces more vapors from a weak solution by using latent heat of vaporization of refrigerant.

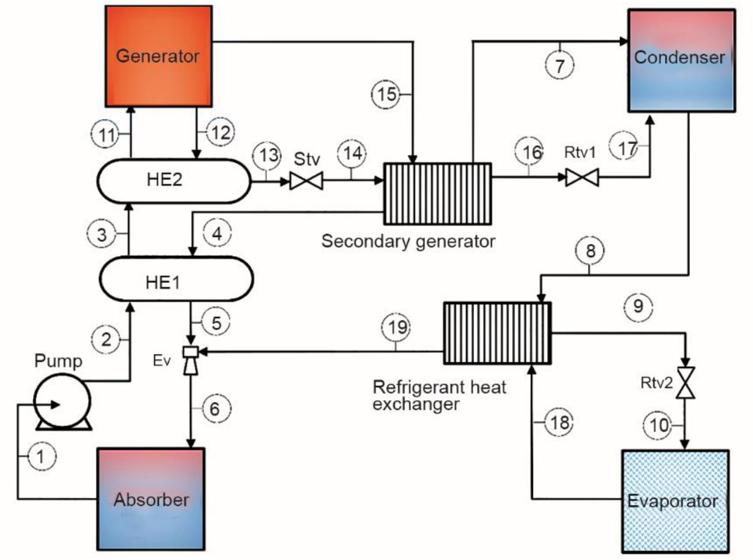

Figure 1. Block diagram of the DVAS

As a result, the weak solution becomes weaker and enters the next solution heat exchanger, HE1, where the transfer of heat between weak and strong solutions takes place. Low temperature vapors coming out of the secondary generator, condensed in the water-cooled condenser. Next passing through the RHE, the refrigerant enters the ejector valve. An ejector is used to maintain an absorber pressure at a level higher than that in the evaporator. Weaker solution coming from HE1 enters the ejector (primary flow of the ejector) and entrains vapors (secondary flow) from the evaporator. The mixed stream is then discharged to the absorber at the pressure of the absorber. A throttle valve is a dissipative integral that assists the other productive component in VAS. The motive fluid is a weak solution that entrains the low pressure refrigerant vapors from the evaporator. Constant pressure evaporation will take place in the evaporator. In this way, the cycle will complete.

Mathematical model description

Mathematical modeling of the proposed model of DVAS is given keeping the conservation of masses, energy, and exergy along with all the components. During the thermodynamic analysis of the DVAS, each component of the system has been acknowledged as control volume with inlet and outlet streams, heat inlet and outlet flow, and/or work:

$$\text{COP} = \frac{\dot{Q}_\text{e}}{\dot{Q}_\text{gen} + \dot{W}_p} \tag{1}$$

$$e_x = (h_x - h_o) - (s_x - s_o) \tag{2}$$

where e_x is the specific exergy of the component corresponding to specific enthalpy, h_x, and specific entropy, s_x. By finding the region in a system where entropy generation occurs and minimizing exergy losses, the overall exergy level of the system can be increased. Second law analysis is based on exergy, e_x, that is maximum possible useful work regarding some dead state in the thermodynamic system with environment temperature, T_o, as:

$$\sum(\dot{m}e)_\text{in} + \sum\left[\dot{Q}\left(1-\frac{T_o}{T}\right)\right]_\text{in} = \sum(\dot{m}e)_\text{out} + \sum\left[\dot{Q}\left(1-\frac{T_o}{T}\right)\right]_\text{out} \pm \sum\dot{W} \tag{3}$$

where e_in is the exergy of flow stream at inlet and e_out is exergy of the current at the outlet, whereas, T is the temperature of the specific component under consideration. Exergy destruction rate for control volume in steady-state is calculated from the difference between incoming and outgoing exergy flows:

$$E\dot{D} = \sum\dot{m}_\text{i}e_\text{i} - \sum\dot{m}_o e_o + \left[\sum Q_\text{i}\left(1-\frac{T_o^{'}}{T_\text{i}}\right) - \sum Q_\text{i}\left(1-\frac{T_o^{'}}{T_o}\right)\right] \pm \dot{W} \tag{4}$$

where $T_o^{'}$ is ambient temperature or dead state temperature, $\dot{m}_\text{i}$ and e_i are mass-flow rate and exergy at inlet, respectively, with inlet temperature, T_i. For a highly efficient system, the irreversibility of the system should be as small as possible. Another important consideration of the absorption system is the cut-off temperature of the absorption system. It is the minimum operating temperature of the system and it depends upon T_a, $T_\text{e,}$ and T_c. These temperatures are correlated by using regression analysis:

$$T_\text{c}' = x_o + x_1 T_\text{c} + x_2 T_\text{c}^2 + x_3 T_\text{a} + x_4 T_\text{a}^2 + x_5 T_\text{e} + x_6 T_\text{e}^2 \tag{5}$$

where x_o, x_1, x_2, x_3, x_4, x_5, and x_6 are coefficients of the eq. (5) given [21]. The previous equation is valid only for defined ranges of temperatures of absorber, evaporator, and condenser as $5 \leq T_\text{e} \leq 15$ °C, $30 \leq T_\text{a}$, and $T_\text{c} \leq 45$ °C.

Entropy and enthalpy correlations for modeling

There are correlations available in the literature to calculate entropy and enthalpy of LiBr-H_2O solution and refrigerant, water, at corresponding temperature, T, pressure, P, and concentration, v. For example, correlations for entropy and enthalpy calculation at the condenser corresponding to its temperature and pressure is:

$$h_c = -B_o + B_1 T - B_2 T^2 + B_3 T^3 + B_4 P - B_5 P - B_6 P T^2 \tag{6}$$

$$S_c = -C_o + C_1 \log(\mathrm{T}) - C_2 \mathrm{T} + C_3 T^2 + C_4 P - C_5 PT + C_6 T \tag{7}$$

Similarly, the correlation for entropy and enthalpy calculation at the evaporator, generator, and secondary vapor generator are available [24]. Specific enthalpy of LiBr-H_2O solution after absorber is calculated using temperature, T [°C] and concentration, v, [%] of the absorbent in solution. Instead of using graphs, can also use these correlations and that can easily model on SIMULINK, MATLAB using THERMOLIB blocks. Specific enthalpy and entropy calculation of weak solution of LiBr-H_2O after solution heat exchanger, the generator is calculated:

$$h = (A_o + A_1 v)T + 0.5(A_2 + A_3 v)T^2 + (A_4 + A_5 v + A_6 v^2 + A_7 v^3) \tag{8}$$

$$s = \sum_{i=0}^{3} \sum_{j=0}^{3} D_{ij} T^i V^j \tag{9}$$

Specific entropy and enthalpy of saturated liquid water, after the rejection of heat of condensation to weak solution for more vapor generation, can be calculated as given [25].

Modelling using THERMOLIB

Simulation is a way of mimicking the actions of the real system. Modeling in THERMOLIB takes place using blocks of components. These blocks do not store mass except tanks and some of the components have inputs and outputs as Q_{dot} and P_{mch} representing energy flows across the border of the block. If correlation equations between variables are known behind the performance of each component for which it is placed, modeling can be performed. Modeling of DVAS using blocks has been done and steady-state analysis has been performed.

Penalty factor method

To choose the more appropriate solution from available all the possible solution is called optimization keeping all the constraints into account. Figure 2 shows the solving method for the Optimization technique for the PFM. The objective function is penalized in PFM for violation of constraints. The penalty factor, P_f, has a large impact on outcomes of the op-

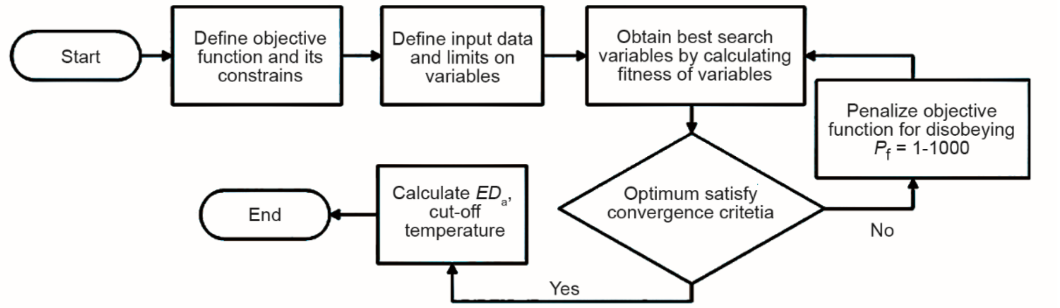

Figure 2. Flow chart diagram for the optimization technique

timization by this method [26]. If all constrained are satisfied then there will be no penalty to the objective function. This optimization technique transforms a constrained problem into an equivalent unconstrained optimization problem by introducing composite objective function (COF) as shown below:

$$\beta = \alpha + P_f \phi^2 \tag{10}$$

Minimizing the COF instead of minimizing objective function by assigning different values of P_f.

After that, keep on changing P_f and reach a point where regardless of the value of P_f almost the same value as the COF. It reveals that COF getting stable with respect to P_f and attains the optimum value of the objective function. Higher value of P_f gives more importance to constrain and slow convergence occurs. The initially small value of P_f is used to get some solution range. Chen and Dai [27] presented in their analysis that the selection of a good penalty parameter will accelerate the convergence of objective function.

Validation of model and comparison

Input variables for the model were considered from Arora and Kaushik [15] study about the double-effect absorption system. Validation of model and data are given in tabs. 1 and 2. The differences in values of heat transfer and exergy destruction rate are less than 6.14% at T_g = 140.6 °C, T_e = 7.2 °C, T_a = T_c = 37.8 °C, $\dot{m}_r$ =1 kg/s, effectiveness of HE = 0.7. The generator operates with a high pressure of 64.47 kPa and a high temperature of 140 °C. The secondary generator and condenser operate with a medium level of pressure *i.e.* 6.558 kPa. Absorber and evaporator operate with low pressure of 1.016 kPa.

Table 1. Comparison and differences of First law analysis results for DVAS

Component	Q [KW]		
	[15]	Present work	Differences [%]
Generator	1868.711	1854	–0.787
Absorber	–2942.175	–2949	0.231
Secondary generator	1272.479	1272	–0.078
Air cooling evaporator	2355.45	2356	0.023
Condenser	–1282.052	–1283	0.073
Pump	0.3598	0.3819	6.142
Solution HE1	518.596	545.8	5.245
Solution HE2	861.206	835.2	–3.019
Energy input	4224.521	4210.38	–0.334
Energy output	4224.227	4232	0.184

Figure 3 shows the same trend of the effect of absorber and condenser temperature on the cut-off temperature of the absorption system as shown by Pandya *et al.* [21].

Table 2. Comparison and differences of Second law analysis results for DVAS

Component	$\dot{E}D_{\min}$ [KW]		
	[15]	Present work	Differences [%]
Generator	721.721	720.97	3.457
Absorber	67.549	67.39	0.235
Secondary generator	12.475	13.21	5.891
Air cooling evaporator	2355.45	2356	0.023

Results

In the DVAS, the enthalpy and entropy values vary due to temperature, pressure, and concentration variations after each component. The exergy destruction rate along all components for DVAS has been calculated. The generator operates with a high pressure of 64.47 KPa and a high temperature of 140 °C. The secondary generator and condenser operate with a medium level of pressure *i.e.* 6.558 KPa. Absorber and evaporator operate with low pressure of 1.016 KPa. The mass-flow rate of refrigerant is considered to be 1 kg/s at the evaporator. Comparison between the results in terms of graph and table given below for a better understanding of optimization results. Updated state points and calculated parameters for proposed DVAS are shown in tab. 3.

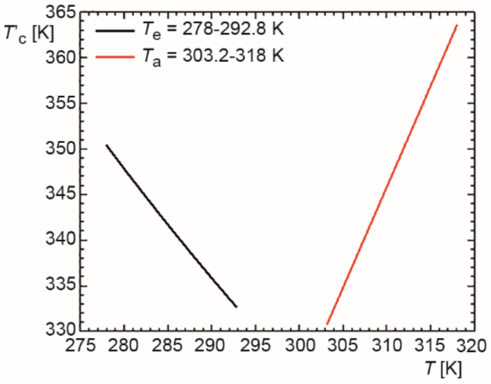

Figure 3. Effect of absorber and evaporator temperature on the cut-off temperature of DVAS [21]

Effect of evaporator temperature and absorber temperature

As the temperature in the evaporator increases, the exergy destruction rate at the absorber also increases. Lower evaporator temperature is desirable for lesser exergy destruction at absorber as shown in fig. 4(a). Lesser exergy destruction rate at the absorber should be attained at some suitable temperature at the evaporator. Similarly, as the temperature in the absorber changes, the exergy destruction rate at the absorber varies. Since the rejection of heat at absorber and condenser takes place with water of streams that are available in a range of 35 °C to 40 °C. Figure 4(b) shows that as absorber temperature increases, the exergy destruction rate at absorber will decrease. But the higher temperature at the absorber decreased the absorbance of the absorbent as declared [22] and the lower temperature at the absorber decreased the cut-off temperature that is desirable in any absorption system.

Effect of the mass-flow rate of weak solution

Figure 4(c) showing the effect of the change of mass-flow rate, $\dot{m}$, of the weak solution on the exergy destruction rate of the absorber $\dot{E}D_a$. A higher mass-flow rate in the absor-

Table 3. State points for the modified model of DVAS with the calculated parameter

State points	T_i [°C]	P_i [KPa]	x_i [kgkg^{-1}]	$\dot{m}_i$ [kgs^{-1}]	h_i [KJkg^{-1}]	S_i [KJkg^{-1}K^{-1}]
1	37.8	1.016	0.5542	9.033	91.88	0.2288
2	37.8	64.47	0.5542	9.033	91.92	0.2288
3	66.15	64.47	0.5542	9.033	149.3	0.4066
4	87.8	6.558	0.62323	8.033	221.2	0.4787
5	53.01	6.558	0.62323	8.033	156.7	0.2905
6	53.01	1.016	0.62323	9.033	421.98	1.272
7	87.8	6.558	0	0.4671	2664	8.58
8	37.8	6.558	0	1	158.3	0.5428
9	25.62	6.558	0	1	105.83	0.3772
10	2.505	1.016	0	1	105.83	9.089
11	111.5	64.47	0.5542	9.033	244.7	0.669
12	138.15	64.47	0.58898	8.5	307.1	0.7672
13	88.14	64.47	0.58898	8.5	205.8	0.5053
14	88.14	6.558	0.58898	8.5	205.8	0.5054
15	138.15	64.47	0	0.533	2755	7.765
16	87.8	64.47	0	0.533	367.7	1.167
17	37.8	6.558	0	0.533	367.7	1.216
18	7.2	1.016	0	1	2514	8.968
19	29.62	1.016	0	1	2553	8.502

ber produces more entropy generation that results in more destruction of the exergy at the absorber as depicted from the graph. The smaller value of the mass-flow rate in the laminar range of fluid-flow is desirable to avoid losses of energy and more entropy generation due to turbulence. So, an optimized value of the mass-flow rate of the weak solution should be set towards the absorber for better performance.

Effect of concentration of LiBr in solution

The concentration of the lithium bromide in solution also disturbs the exergy destruction rate at the absorber as LiBr is hygroscopic [5]. A large quantity of the LiBr causes more bond formation with the refrigerant vapors during mixing as a result more heat is generated in the absorber causing higher heat losses to the environment [21].

Mass-flow rate and percentage of the LiBr in solution has less impact on the exergy destruction rate at absorber as compared to temperature variations of the absorber and evaporator as shown in fig. 4(e). So, by considering some suitable values of mass-flow rate and concentration, the optimum value of absorber and evaporator temperature has been obtained using PFM to get the optimum cut-off temperature with a lesser exergy destruction rate at absorber.

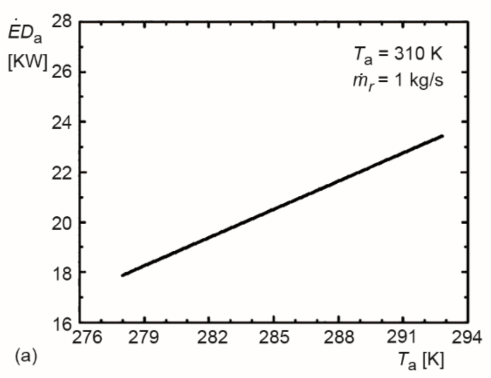

Figure 4(a). Effect of evaporator temperature on exergy destruction rate at absorber

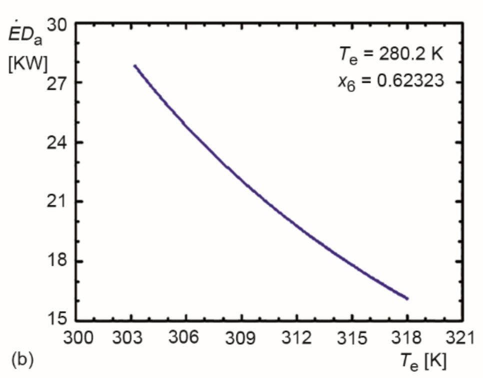

Figure 4(b). Effect of absorber temperature on exergy destruction rate at absorber

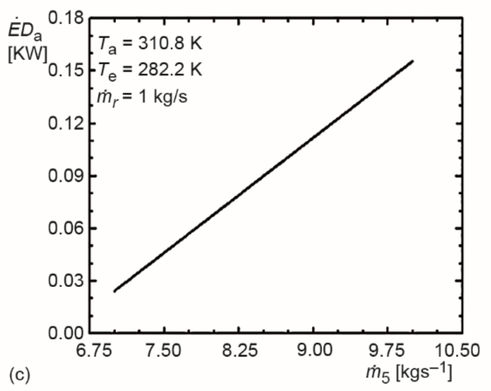

Figure 4(c). Effect of the mass-flow rate of weak solution on exergy destruction rate at absorber

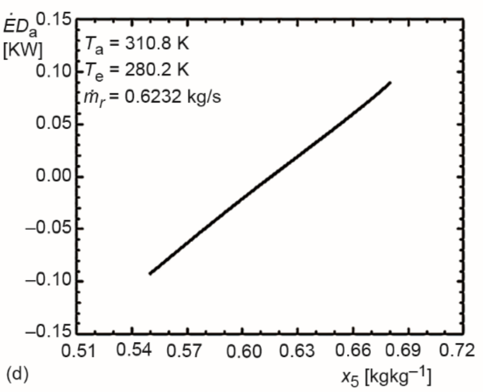

Figure 4(d). Effect of concentration of LiBr in solution on exergy destruction rate at absorber

Comparison between results

By energy and exergy analysis of the double-effect vapor absorption system with ejector and refrigerant heat exchanger, calculated parameters are given in tabs. 4 and 5. It considers that the absorber and condenser temperature, *i.e.* $T_a = T_c$, variation from 30.2 °C to 45 °C and evaporator temperature, T_e, variant from 5 °C to 15 °C with a step size of 0.5 °C then there comes an optimum situation after implementing PFM at T_c = 35.8 °C, T_e = 5.1 °C. and when the exergy destruction rate is minimum *i.e.* 45.525 °C by assuming penalty factor P_f = 1 as given in tab. 6 and bar chart given in fig. 5. But in this situation, there is a compromise with cut-off temperature *i.e.* 104.8930 °C, *i.e.* higher value

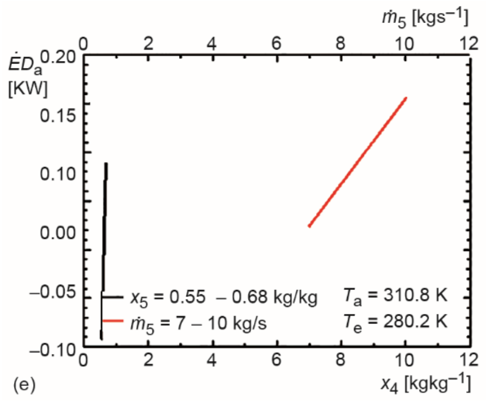

Figure 4(e). Effect of mass-flow rate and concentration of the weak solution on exergy destruction rate at the absorber

of cut-off temperature. Table 6 has been set by optimizing eq. (12) by considering eq. (11) as constraining for the main function, *i.e.* $\dot{E}D_a$.

$$\phi_1 = T_c' - 91.8962\ ^\circ\text{C} \tag{11}$$

$$\beta = \dot{E}D_a + P_f \phi^2 \tag{12}$$

By changing the value of penalty factor and calculating results, function to be stationary at T_e = 5.1 °C and T_a = 35.8 °C where the results satisfying convergence criteria and $\dot{E}D_a$ = 61.623 KW with T_c' = 84.4974 °C.

Table 4. The First law analysis results for DVAS

Component	[15]	Present work		
		With ejector $\dot{Q}$ [KW]	With RHE $\dot{Q}$ [KW]	With ejector and RHE $\dot{Q}$ [KW]
Generator	1868.71	1868.69	1868.69	1868.69
Absorber	2942.17	2664.82	2961.81	2664.82
Secondary generator	1272.47	1272.11	1272.11	1272.11
Air cooling evaporator	2355.45	2356.01	2408.17	2408.17
Condenser	1282.05	1283.01	1283.01	1283.01
Pump	0.3598	0.3819	0.3819	0.3819
Solution heat exchanger 1	518.59	545.81	545.81	545.81
Solution heat exchanger 2	861.20	835.21	835.21	835.21
Energy input	4224.52	4225.10	4277.26	4277.24
Energy output	4224.22	3947.83	4244.81	3947.01
COP	1.26	1.26	1.29	1.288

For the tables, the minimum exergy destruction rate at absorber is the main objective function and β is a composite function. To get the minimum value of exergy destruction rate at absorber, minimize β by using a different value of P_f in such a way that eq. (12) becomes stable with respect to P_f. It means our objective function is minimized accounting for the constrained, ϕ, of the cut-off temperature. An initially small value of penalty factor has been used to gain a suitable range of input data by giving less importance to constrain as can see large variations in cut-off temperature *i.e.* constrained of the COF. Progressively objective function has been more penalized by giving a higher value of P_f for disobeying the constrained. In the end situation, values of COF more or less the same regardless of the value of P_f. That means COF is stationary with respect to scalar *i.e.* P_f from tab. 6, it is concluded that a lower value of exergy destruction rate can be obtained on the cost of higher cut-off temperature.

Using an optimization technique and improvement in the model, an optimized solution is given in fig. 5. By changing the evaporator temperature to value 5.1 °C, get 8.77% lower exergy destruction rate at absorber with too much lesser cut-off temperature *i.e.*

Table 5. The Second law analysis results for DVAS

Component	[15]	Present work $\dot{E}D$ [KW]		
		With ejector	With RHE	With ejector and RHE
Generator	21.721	20.97	20.97	20.97
Absorber	67.549	67.39	67.39	67.39
Secondary generator	12.475	13.21	13.21	13.21
Air cooling evaporator	86.275	90.123	84.118	90.123
Condenser	3.086	3.083	3.083	3.083
Solution heat exchanger 1	28.056	27.89	27.89	27.89
Solution heat exchanger 2	43.1	42.8	42.8	42.8
Refrigerant throttle valve 1	7.813	7.798	7.798	7.798
Refrigerant throttle valve 2	6.936	7.002	7.002	7.002
Solution throttle valve 1/ejector valve	0.0236	0.021	0.0236	0.021
Solution throttle valve 2	0.249	0.243	0.243	0.243
Energy loss at absorber, $\dot{E}_{\mathrm{L,a}}$	121.112	109.71	121.97	109.74
Energy loss at condenser, $\dot{E}_{\mathrm{L,c}}$	52.775	52.775	52.83	52.83
Total irreversibility in cycle	173.887	162.485	174.809	162.578
Exergy input	514.45	514.43	514.65	514.65
Exergy output	63.277	63.222	105.38	105.38
Exergetic efficiency	12.3	12.2	20.42	20.42

Table 6. Minimum exergy destruction rate at absorber by using PFM $\phi_1 = T_c'$-91.8962 °C

P_f	T_e [°C]	$T_c = T_a$ [°C]	$\dot{E}D_{\min}$ [KW]	T_c' [°C]
1	5.1	45	45.525	104.8930
2	5.1	44.6	53.718	104.8931
3	5.1	43.1	54.724	100.6739
5	5.1	40.6	55.701	95.12787
10	5.1	38.4	56.562	90.2526
50	5.1	36.3	57.371	85.6036
100	5.1	36.1	57.484	85.1611
500	5.1	35.8	60.575	84.4974
1000	5.1	35.8	61.584	84.4974
2500	5.1	35.8	61.623	84.4974

84.497 °C. That is the improvement in the modified model to get better results at a lower amount of energy loss to the environment. By using the liquid-vapor ejector, the temperature at the absorber is controlled keeping the constraint of cut-off temperature into account. The RHE lessened the temperature at an evaporator that is desirable for the lesser value of exergy destruction rate at absorber and improved performance.

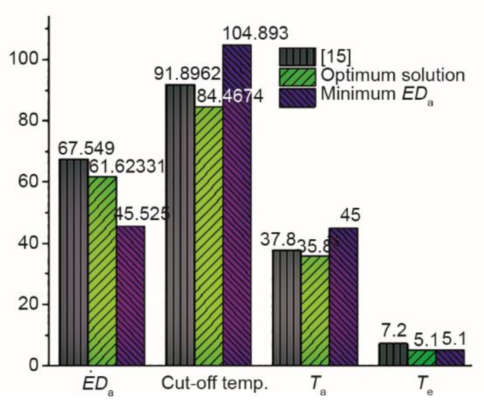

Figure 5. Comparison of three different scenarios; (a) [15], (b) optimum solution, and (c) minimum $\dot{E}D$ at the absorber

Conclusion

The present study provides the optimum operating temperature for DVAS with lower exergy loss at the absorber. It concluded as follows.

- The RHE after the evaporator takes the heat from the refrigerant to decrease the temperature gradient between refrigerant vapors and weak solution at the absorber, its consequences in lesser entropy generation and lesser exergy loss and also improved the COP by 2.4%.
- An optimized solution to the problem has been obtained (Te = 5.1 oC, Ta = 35.8 oC, T′c = 84.497 oC) as the presented model radiated 9.4% lesser exergy loss at absorber and exergetic efficiency of the system improve by 8.2%.
- By liquid-vapor ejector, the temperature at the absorber is controlled keeping the constraint of cut-off temperature into account. The decrease cut-off temperature from 91.89 $^{\circ}$C to 84.497 $^{\circ}$C has also been observed with lesser heat losses at the absorber. The lower cut-off temperature (*i.e.* the minimum temperature at which the boiling starts in the generator) of the VAS enables us to operate systems on a lower energy supply like the solar collector.
- Using this technique, energy can be recovered in many thermodynamic systems like vapor compression systems, steam power plants, *etc.* with the help of modeling in THERMOLIB. The multi-effect absorption system shows better performance by optimizing the operating parameter which results in minimizing the irreversibility to 61.623 KW.

Nomenclature

$\dot{E}D$ – exergy destruction rate, [W]
E_L – exergy loss, [W]
E_v – ejector valve
e_x – specific exergy, [J]
g_{sec} – secondary generator
P_f – penalty factor
P_o – reference pressure, [Pa]
$\dot{Q}$ – heat flow, [W]
T'_c – cut-off temperature at generator, [K]
T_o – reference temperature, [K]
$\dot{W}_p$ – work required at the pump to force the rich mixture towards the generator
x – kg of absorbent per kg of solution

Greek symbols

α – objective function
β – composite objective function
ϕ – constrained to objective function

Subscripts

a – absorber
c – condenser
e – evaporator
g – primary generator
i – inlet
min – minimum
o – outlet

Acronyms

COF – composite objective function
DVAS – double-effect vapor absorption system
Non-OECD – non-members organization for economic cooperation and development
PFM – penalty factor method
RHE – refrigerant heat exchanger
TEWI – total equivalent warming impact
VAS – vapor absorption system

Reference

[1] Alexander, P. C., Energy Consumption and Heat Recovery of Refrigeration System in Modern Arena, *Johnson Controls Building Efficiency*, Denmark, p. 6, 2009
[2] Florides, G. A., *et al.*, Modelling, Simulation and Warming Impact Assessment of a Domestic-Size Absorption Solar Cooling System, *Appl. Therm. Eng.*, *22* (2002), 12, pp. 1313-1325
[3] Liu, C., *et al.*, Investigation of Thermal and Optical Performance of a Phase Change Material-Filled Double-Glazing Unit, *J. Build. Phys.*, *42* (2018), 2, pp. 99-119
[4] Li, *et al.*, D., Thermal Performance of a PCM-Filled Double Glazing Unit with Different Optical Properties of Phase Change Material, *Energy Build.*, *119* (2016), May, pp. 143-152
[5] Siddiqui, M. A., Optimum Generator Temperatures in Four Absorption Cycles Using Different Sources of Energy, *Energy Convers. Manag.*, *34* (1993), 4, pp. 251-266
[6] Asdrubali F., Grignaffini, S., Experimental Evaluation of the Performances of a H_2O-LiBr Absorption Refrigerator Under Different Service Conditions, *Int. J. Refrig.*, *28* (2005), 4, pp. 489-497
[7] Kumar, B., *et al.*, Thermodynamic Analysis of a Single Effect Lithium Bromide Water Absorption System Using Waste Heat in Sugar Industry, *Thermal Science*, *22* (2018), 1, pp. 507-517
[8] Farshi, L. G., *et al.*, Thermodynamic Analysis and Comparison of Combined Ejector – Absorption and Single Effect Absorption Refrigeration Systems, *Appl. Energy*, *133* (2014), Nov., pp. 335-346
[9] Vereda, C., *et al.*, Study of an Ejector-Absorption Refrigeration Cycle with an Adaptable Ejector Nozzle for Different Working Conditions, *Appl. Energy*, *97* (2012), Sept., pp. 305-312
[10] Sozen, A., Ozalp, M., Performance Improvement of Absorption Refrigeration System Using Triple-Pressure-Level, *Appl. Therm. Eng.*, *23* (2003), 13, pp. 1577-1593
[11] Chen, L.-T., C., A New Ejector-Absorber cycle to Improve the COP of an Absorption Refrigeration System, *Appl. Energy*, *30* (1988), 1, pp. 37-51
[12] Azhar, M., Siddiqui, M. A., Optimization of Operating Temperatures in the Gas Operated Single to Triple Effect Vapour Absorption Refrigeration Cycles, *Int. J. Refrig.*, *82* (2017). Oct., pp. 401-425
[13] Gomri, R., Hakimi, R., Second Law Analysis of Double Effect Vapour Absorption Cooler System, *Energy Convers. Manag.*, *49* (2008), 11, pp. 3343-3348
[14] Khaliq, A., Kumar, R., Exergy Analysis of Double Effect Vapour Absorption Refrigeration System, *Int. J. Energy Res.*, *32* (2008), 4, pp. 161-174
[15] Arora, A., Kaushik, S. C., Theoretical Analysis of LiBr/H_2O Absorption Refrigeration System, *Archives of Thermodynamics*, *33* (2012), 4. pp. 23-40
[16] Rostami, S., *et al.*, Exergy Optimization of a Solar Collector in Flat Plate Shape Equipped with Elliptical Pipes Filled with Turbulent Nanofluid Flow: A Study for Thermal Management, *Water (Switzerland)*, *12* (2020), 8, 2294
[17] Mitrovic, M. D., *et al.*, Exergy and Exergoeconomic Analysis of a Steam Boiler, *Thermal Science*, *22* (2018), Suppl. 5, pp. S1601-S1612
[18] Ben Jemaa, R., *et al.*, Experimental Investigation and Exergy Analysis of a Triple Fluid Vapor Absorption Refrigerator, *Energy Convers. Manag.*, *124* (2016), Sept., pp. 84-91
[19] Azhar, M., Siddiqui, M. A., Energy and Exergy Analyses for Optimization of the Operating Temperatures in Double Effect Absorption Cycle, *Energy Procedia*, *109* (2017), Mar., pp. 211-218
[20] Rostamzadeh, H., *et al.*, Exergoeconomic Optimisation of Basic and Regenerative Triple-Evaporator Combined Power and Refrigeration Cycles, *Int. J. Exergy*, *26* (2018), 1-2, pp. 186-225
[21] Pandya, B., *et al.*, Thermodynamic Evaluation of Generator Temperature in Libr-Water Absorption System for Optimal Performance, *Energy Procedia*, *109* (2017), Mar., pp. 270-278

[22] Nikulshin, V., *et al.*, Thermodynamic Analysis of Air Refrigerator on Exergy Graph, *Thermal Science*, *10* (2006), 1, pp. 99-110
[23] Andi, B., *et al.*, Experimental Analysis of Triple Fluid Vapour Absorption Refrigeration System Driven by Electrical Energy and Engine Waste Heat, *Thermal Science*, *23* (2019), 5, pp. 2995-3001
[24] Talbi, M. M., Agnew, B., Exergy Analysis: An Absorption Refrigerator Using Lithium Bromide and Water as the Working Fluids, *Appl. Therm. Eng.*, *20* (2000), 7, pp. 619-630
[25] Saul, A., Wagner, W., International Equations for the Saturation Properties of Ordinary Water Substance, *J. Phys. Chem. Ref. Data*, *16* (1987), 4, pp. 893-901
[26] Zhao, X., *et al.*, A MILP Model Concerning the Optimisation of Penalty Factors for the Short-Term Distribution of Byproduct Gases Produced in the Iron and Steel Making Process, *Appl. Energy*, *148* (2015), June, pp. 142-158
[27] Chen, Z., Dai, Y., A Line Search Exact Penalty Method with Bi-Object Strategy for Non-Linear Constrained Optimization, *J. Comput. Appl. Math.*, *300* (2016), July, pp. 245-258

Paper submitted: October 16, 2020
Paper revised: May 15, 2021
Paper accepted: May 21, 2021

© 2022 Society of Thermal Engineers of Serbia.
Published by the Vinča Institute of Nuclear Sciences, Belgrade, Serbia.
This is an open access article distributed under the CC BY-NC-ND 4.0 terms and conditions.